

CHAPTER IV
PROCESS OPTIMIZATION OF ELECTROSPUN SILK FIBROIN FIBER
MAT FOR ACCELERATE WOUND HEALING

4.1 ABSTRACT

With the outstanding biocompatibility of *Bombyx mori* silk fibroin, this study is designed to fabricate biomimetic nanofibrous structure of a silk fibroin which have opportunity to enhance cell activities for tissue formation. The electrospinning of blend silk fibroin with low molecular weight poly(ethylene-oxide) (PEO) is explored with ease of preparation for high productivities. The average diameter of eSF is decreased from 414 ± 73 nm to 290 ± 46 nm after PEO extraction. To induce the desired cellular activity, the surface of the eSF fibers is modified with fibronectin by using the carbodiimide chemistry method. The potential use of as the obtained wound healing material is assessed by indirect cytotoxicity evaluation on normal human dermal fibroblast (NHDF) in terms of their attachment and proliferation of the cells. The surface-modified eSF nanofiber mats show the best support for cellular adhesion and spreading as a result of fibronectin grafting on the fiber surface, especially for cell migration inside the fibrous structure. These results demonstrate that this process can provide a new fabrication technique of surface-modified silk fibroin electrospun nanofibers for biomedical application; with the ability to accelerate wound healing.

Keywords: Electrospinning; Fiber mat; Silk fibroin; Fibronectin; Wound dressing

4.2 Introduction

Nowadays, there are numerous researches regarding to the relative efficiency of the various kinds of material for effective wound healing. Biopolymers and fabrication techniques have been studied not only for covering in order to prevent infection but also have extraordinary properties which promote the healing process [1-3]. Generally, the wound healing process can be divided into 3 phases: inflammation, proliferation, and tissue remodeling [1]. The healing process is a complicated system that involves the interaction of many types of cells. Fibroblasts are one of the most abundant cell types in connective tissues which become activated and can differentiate into myofibroblasts when tissues are injured [4]. The ideal candidate for promotion of wound healing should mimic the structure and biological environment of the wounds, i.e., native extracellular matrix (ECM) proteins, which provide support and biological functions for cellular activities [5]. To meet such specification, it is necessary to choose the appropriate biomaterial for the fabrication of nanofibrous scaffold for tissue engineering.

Domesticated, *Bombyx mori*, silkworms are widely available in Thailand which is well known in the textile industry for centuries. Silk fibroin (SF) from the silk cocoon is generally defined as an attractive biomaterial because of its unique characteristics such as high mechanical strength, excellent biocompatibility, controllable structure and morphology, and wide variety of constructive properties on tissue engineering [6-9]. The fibroin fibers are composed of three proteins: a heavy chain (~350 kDa), a light chain (~25 kDa), and small glycolprotein (~30 kDa). The light chain fibroin exhibits the best properties — higher hydrophilicity, water uptake ability, low degradation rate, and superior cell adhesion properties. This may then introduce its potential uses as has been previously reported (e.g. films, foams, hydrogels, sphere, and fibers) [8-10]. The amino acid composition of silk fibroin from *B. mori* consists primarily of glycine (43 %), alanine (30 %) and serine (12 %), which composed of repeated motifs, [GAGSGA]_n in the crystalline domain [9, 11, 12]. In addition, major interest of silk fibroin for wound dressing application is due to the fact that silk can be engineered to degrade at slow rate due to its high crystallinity induced by β -sheet structure formation. Therefore, the slow degradation

of silk mats will not cause any inflammatory reaction and interference with healing process [20].

Biomaterial-scaffold design is an important element for tissue engineering. Electrospinning is of interest in this study since it can produce non-woven nanofibers mat which unique three-dimensional structure that mimics the topographic features and biological function of collagen structure in natural ECM [5]. The important advantages of electrospinning technique are that it can generate loose porous fibrous membrane with high porosity and surface area, which can be an excellent candidate for many biomedical applications ranging from drug delivery, tissue engineering, implants, and wound dressing. Numerous researches of Silk fibroin electrospun were focused on the preparation of electrospinning solution that usually prepared in formic acid to producing cylindrical or ribbon like fibers where they demonstrated good biocompatibility with a variety of cell [6, 16, 18, 21, 26]. Electrospun silk fibroin can be produced in a wide range of diameters from a few nanometers to micrometers depending on the process. The effect of silk solution viscosity, cause of solution concentration, was the most important factor on morphology and fibers diameter. From our previous report, electrospun silk fibroin prepared by formic acid has the fiber diameters ranging between 210 to 670 nm [18]. Consequently, electrospinning of composite material based on silk fibroin were also studied such as poly(ethylene oxide) (PEO, 900 kDa) which was used as additive viscosity of aqueous silk fibroin solution, yielding the uniform electrospun fiber with significantly diameter ranging in sub-micron [15, 19, 22, 24, 27, 28]. Almost all of PEO could be removed by subsequently washing the fiber with water after induction of β -sheet formation to reduce toxicity. Beyond that, introducing adsorption and chemical immobilization of protein, such as BMP-2, RGD, and fibronectin, has been explored as cellular binding sites for integrin receptors and impact cellular adhesion and proliferation [9, 19, 22, 28, 29].

In this study, we aimed to optimize the preparation process for ultra-fine eSF fibers. Electrospinning from blends of Thai silk fibroin in aqueous solution were study in order to achieve the effective ingredient for electrospinning. The concentration effects of low molecular weight PEO (600 kDa) and relative humidity on morphology were investigated prior to PEO extraction. The surface

immobilization of fibronectin, which is play a major role in physiological process, on eSF was carried out by wet chemical method to improve cellular spreading. The potential for use eSF fiber mats as wound dressing was evaluated by *in vitro* cellular respond using human fibroblasts, in which the attachment and proliferation activities were investigated.

4.3 Experimental details

4.3.1 Materials

Fresh Thai silk cocoons of *Bombyx mori* silkworms (Chul 1/1) were generously provided by Chul Thai Silk (Phetchabun, Thailand). Poly(ethylene oxide) (PEO, 600 kDa) was purchased from Acros organics. One-ethyl-3-(dimethylaminopropyl) carbodiimide hydrochloride (EDC), N-hydroxysuccinimide (NHS) and fibronectin were purchased from Sigma (Sigma, USA). The chemicals used for the preparation of SF and its spinning solutions were sodium carbonate (Na_2CO_3), lithium bromide (LiBr), were purchased from Riedel-de Haën (Germany). Others chemicals used in cell study were purchased from Invitrogen Corp., (USA). All chemicals were of analytical grade and used without further purification.

4.3.2 Preparation of Electrospinning Solution

Thai *B. mori* silk cocoons were degummed by boiling in an aqueous solution of 0.02 M Na_2CO_3 for 30 min three times, and then rinsed with warm distilled water to get rid of sericin proteins. Silk fibroin was extracted from the degummed silk treads by dissolved in 9.3 M LiBr (55 °C) for 30 min at a final concentration of approximately 10 % (w/v). The solution was dialyzed in distilled water using dialysis tubing cellulose membrane (Sigma-Aldrich, USA) for 3 days. The dialysate was centrifuged at 5 °C for 20 min. The SF solution was filtered and lyophilized by using LABCONCO: FreezeZone 6 to obtain the regenerated SF sponges. SF/PEO blend in aqueous solution was used for electrospinning. The SF sponges and PEO (600 kDa) was mixed at various weight ratios and stirred for 12 h at room temperature. The electrospinning solution was prepared at 10 % (w/v) of SF/PEO blending concentration.

4.3.3 Preparation of Electrospun SF Nanofibers via Electrospinning

During electrospinning process, a homogeneous solution of SF/PEO was contained in a 20 ml glass syringe. A high electric potential in the range of 12-14 kV was applied to a droplet of the solution at a tip of a gauge 20 syringe needle. A jet of the silk fibroin solutions was ejected to a grounded rotating drum with aluminum foil attached. The distance between the tip of the needle and the drum was fixed at 10 cm. The syringe and the needle were tilted $\sim 45^\circ$ to maintain the flow rate of the electrospinning solution at the tip of the needle. The electrospun nanofibers were processed under the various relative humidity in the range from 30-60 % at the ambient temperature. The suitable condition was chosen for electrospinning to obtain nanofiber mats.

4.3.4 Fibers Treatment and Surface Modification of eSF

The water soluble of SF/PEO fiber mats were immerse in 98 % methanol for 10 minute and air dried to induce the conformation from amorphous (unstable silk I) to β -sheet transition (silk II) which was water-insoluble. Treated fiber mats were washed in distilled water at 37 °C for 3 days to remove PEO. The PEO extracted silk fibroin fiber mats were put into a PBS buffer for 30 min to hydrate and stimulate the -COOH groups on aspartic and glutamic residues on the surface of eSF. Then the fibers were reacted by reaction with 1-ethyl-3-(dimethylaminopropyl) carbodiimide hydrochloride (EDC)/ N-hydroxysuccinimide (NHS) solution (0.5 mg/mL of EDC with 0.7 mg/mL of NHS in PBS buffer) for 15 min at room temperature to create activated functional group on the surface. The activated fiber mats were rinsed with PBS buffer, then treated with 0.1 mg/ml fibronectin in the PBS for 2 h at ambient temperature and rinsed with PBS buffer for 3 times followed by distilled water to get rid of excess peptide and salts before air-dried [29, 30].

4.3.5 Scanning Electron Microscopy

Hitachi S-4800 Ultra-high resolution cold Field Scanning Electron Microscope (FE-SEM) was used to observe morphology and size of the electrospun fibers by operating at 10 kV. The samples were attached carefully on the stub, and then sputter coated with platinum before analysis. The fibers sizes were determined by measuring randomly from SEM images by using SemAphore 4.0 program.

4.3.6 Fourier Transform Infrared Spectroscopy (FTIR)

All Infrared spectra of electrospun fibers were recorded by using Thermo Nicolet Nexus 670 Spectrophotometer. Each spectrum was recorded by accumulation of 32 scans with a resolution of 4 cm^{-1} in a range of 400 to $4,000\text{ cm}^{-1}$. The measurement was achieved by using ZnSe crystal cell with an attenuated total reflectance fourier transform (ATR-FTIR) mode.

4.3.7 Water Retention and Dissolution Behavior

Both of electrospun fiber mats were completely dried at $60\text{ }^{\circ}\text{C}$ for 24 h, prior to storage in the desiccators overnight to equilibrium to observe the initial dry weight (W_i) of both of fiber specimens. At designed time points, both of electrospun fiber mats were immersed in PBS buffer at $37\text{ }^{\circ}\text{C}$. The wet weight of the fiber mats (W_f) was determined after the elimination of excess water. The water content of the electrospun fiber mats were calculated as follows:

$$\text{Water content (\%)} = (W_f - W_i) / W_i \times 100$$

The fiber mats then were dried to constant weight at $50\text{ }^{\circ}\text{C}$ for 24 h prior to storage in desecrator overnight. The final dry weight (W_d) after specified time of incubations was recorded to calculate to the percentages of remaining weight as follow:

$$\text{Mass remaining (\%)} = 100 - (W_i - W_d) / W_i \times 100$$

4.3.8 X-ray Photoelectron Spectroscopy (XPS)

To study the grafting efficiency of the eSF, the analysis was carried out by using a Thermo Fisher Scientific Thetaprobe XPS, Singapore. Monochromatic Al $K\alpha$ X-ray was employed for analysis of one spot on each sample with photoelectron take-off angle of 50° (with respect to surface plane). The analysis area was approximately $400\text{ }\mu\text{m} \times 400\text{ }\mu\text{m}$, while the maximum analysis depth lay in the range of $\sim 4\text{-}8\text{ nm}$. A special designed electron flood gun with a few eV Ar^+ ion was used for the charge compensation. Further correction was made based on adventitious C 1s at 285.0 eV using the manufacturer's standard software. Survey

spectra were acquired for surface composition analysis with Scofield sensitivity factors.

4.3.9 Indirect Cytotoxicity Evaluation

Cytotoxicity of the neat and surface-modified eSF with fibroin was evaluated by an indirect method, adapted from the ISO 10993-5 standard test method, by using normal human dermal fibroblasts (NHDF, 15th passage). The cells were incubated in Dulbecco's modified Eagle's medium (DMEM) by adding a requisite amount of 10 % fetal bovine serum (FBS), 1 % l-glutamine, 1 % antibiotic and antimycotic formulation which contained penicillin G sodium, streptomycin sulfate, and amphotericin B. For the cell culture, the specimens were sterilized by UV radiation for about 2 h. They were then immersed in a serum-free medium (SFM; DMEM containing 1 % l-glutamine, 1 % lactalbumin and 1 % antibiotic and antimycotic formulation) for 24 h at the extraction ration of 5, 10 and 20 mg/ml, and then the fiber mats were remove from the medium which were used for cell culture study. The cells of NHDF were cultured separately in 24-well tissue-culture polystyrene plates (TCPS) at 10,000 cells/well in DMEM for 24 h. The medium was replaced with each of extraction medium and re-incubated for 24 h. The cell viability was assessed by using 3-(4,5-dimethylthiazol-2-yl)-2,5-diphenyltetrazolium bromide (MTT) assay. The viability of the cell with fresh SFM was used as control.

4.3.10 Cell Attachment and Proliferation Test

For the cell attachment study, both the neat and modified eSF fiber specimens (about 1.4 cm in diameters) were sterilized by UV radiation about 1 h for each side. The specimens were then placed in 24-well TCPS. The normal human dermal fibroblasts cells were then cultured on the surface of both fiber mats and in glass slides (i.e., positive control) for 2, 4 and 8 h and then incubated in 5 % CO₂ at 37 °C. For the cell proliferation study, the cells, after having been allowed to attach on the substrates for 24 h, were cultured for 1, 2, and 3 days. After each cell-culturing time point, the viability of the attached and proliferated cells was determined by MTT assay

4.3.11 Morphological Observation of Cultured Cells

The cell morphology changed with time on the eSF fiber mats was characterized by FE-SEM. After the culture medium had been removed, the cell-

cultured fiber mats were rinsed twice with PBS and the cells were then fixed with 3 % glutaraldehyde/PBS solution (Electron Microscopy Science, USA) for 30 min. After fixation of cells, the cell-cultured specimens were rinsed again with PBS, prior to being dehydrated at various concentrations of ethanol aqueous solution (i.e., 30, 50, 70 and 90 % v/v) and, finally, with pure ethanol for 2 min each. The specimens were then dried in 100% hexamethyldisilazane (HMDS; Sigma-Aldrich, USA) for 5 min and later dried in air after the removal of HMDS. After being completely dried, the specimens were affixed on stubs and sputter coated with platinum before observing by FE-SEM. For comparison, the morphology of the cells that had been seeded or cultured on a glass substrate (covered glass slide, 1 mm in diameter; Menzel, Germany) was used as positive control

4.3.11 Statistics and Data Analysis

All of the quantitative data were presented as means±standard deviations. Statistical comparisons were carried out by the one-way analysis of variance (one-way ANOVA) with SPSS 13.0 for Windows software (SPSS, USA). The statistical significance was considered at p values < 0.05.

4.4 Results and Discussion

4.4.1 Physicochemical of Neat eSF and Surface-modified eSF Fiber Mats

At 10 wt% Silk/PEO aqueous solutions, the electrospun silk fibroin fibers (eSF) were prepared under different weight ratio of aqueous SF/PEO blends (i.e., 50:50 to 90:10 weight ratio of SF:PEO) in order to fabricate into electrospun fibers. The electrospinning of these solutions were carried out at EFS of 12-14 kV and 15 cm from the slow-rotating cylindrical drum as a collector under different relative humidity. Figure 4.1 shows the morphology of electrospun SF/PEO that was obtained by FE-SEM. At 60 % RH, a large number of beaded fibers were obtained with the decreasing of PEO concentration (i.e., in the range of 70:30 to 90:10 weight ratio of SF:PEO) while electrospinning below 30 % RH results in uniform and bead-free fibers in every concentration. After MeOH treatment and PEO extraction, the obtained fibers at blended PEO concentration lower than 70:30 of SF:PEO can be still in fibers form. Therefore, the fibers prepared at aqueous 70:30 SF/PEO blend

(<30 % RH) were selected for further experiment, because the higher SF concentration resulted in larger fiber diameters.

Figure 4.2 shows the morphology and distribution of eSF fibers obtained in each condition. The removal of PEO did not affect the fiber morphology but significantly changed in average fiber diameter at 70:30 weight ratio of SF:PEO. The average diameter of as-spun SF/PEO fibers is 407 ± 60 nm. The average fiber diameter increased slightly to 414 ± 73 nm after methanol treatment as a result of α -helix to β -sheet transition while retaining integrity and smoothness on the fiber. However, the average fiber diameter is reduced to 290 ± 46 nm without changing the overall morphology after PEO extraction, where FTIR results showed that no PEO is left in the fibers. The PEO extracted eSF fibers showed an even fiber size distribution which means that PEO solution was homogeneously distributed during the preparation phase. Further surface modification also yielded smooth continuous fibers that were 270 ± 44 nm in diameter.

The FT-IR spectra which is well known to be a sensitive method to confirm the chemical conformation, Figure 4.3 shows that after MeOH treatment, the strong absorption bands of amide I (C=O stretching) and amide II (N-H deformation and C-N stretching) at 1642 cm^{-1} and 1532 cm^{-1} shifted to 1622 cm^{-1} and 1512 cm^{-1} respectively which indicated the structure conformation from α -helix or random coil to β -sheet conformation transition [27]. Washing of treated the eSF fiber mats at 37°C for 3 days, resulted in extraction of PEO which show the essential absence of distinctive PEO peak at 1109 cm^{-1} (C-O stretching), 963 cm^{-1} (C-H out of plane) and 843 cm^{-1} (C-H out of plane) [19].

After surface modification, the existing of fibronectin on the surface of eSF fibers mat by using EDC/NHS coupling reaction was further evaluated. There was a contributing absorption peak corresponding to the carbonyl (C=O stretching) at 1663 cm^{-1} . Additionally, the absorption of a broad peak in the range of $3000\text{-}3600 \text{ cm}^{-1}$ corresponding to the N-H stretching of the NH_2 group further confirmed the successful immobilized of the fibronectin on the surface of eSF fiber mats [31]

4.4.2 Surface Elemental Composition

The XPS spectra show the elemental components of neat and surface-modified eSF fibers on the surface. The typical peaks of C 1s, N 1s and O 1s were

obviously observed at 284.6 ± 0.2 eV, 398.3 ± 0.2 eV, and 531.0 ± 0.2 eV of binding energy, respectively [29]. The results of elemental concentrations (in at.%), the N/C, O/C ratios and chemical functions (at.%) of surface before and after modification are reported in Table 1. In comparison, the carbon (C), nitrogen (N) and oxygen (O) elemental compositions (in at.%) in the eSF fibers surface are 67.4 %, 9.5 % and 23.2 %, while the surface-modified eSF by fibronectin are 63.6 %, 16.0 %, and 20.4 % respectively. The increasing of N/C ratio was obviously observed after modification. Nonetheless, the chemical reaction was also investigated by monitoring the components from curve fitting in C1s photoelectron peaks. Figure 4.4 shows three components in C 1s peak which were found in both types of fibers. The components are assigned as: $\underline{\text{C}}-(\text{C,H})$ centered at 285.0 ± 0.2 eV, $\underline{\text{C}}-(\text{O,N})$ centered at 286.5 ± 0.2 eV, and $\text{O}-\underline{\text{C}}=\text{O}$ centered at 288.1 ± 0.2 eV [32]. According to the coupling reaction, a decrease in percentage of $\underline{\text{C}}-(\text{O,N})$ was found which assigned to the carboxylate functions of the silk fibroin protein. Simultaneously, the $\text{O}-\underline{\text{C}}=\text{O}$ and $\underline{\text{C}}-(\text{C,H})$ was significantly increased that may be originated from side chains of amino acids of the coupling of fibronectin on the fiber surface. The data obtained from O 1s and N 1s were in agreement with the C 1s information.

4.4.3 Water Retention and Dissolution Behavior

To study the potential used of fiber mats that required a directly contact with wound exudates, water absorption behavior and dissolution of eSF fiber mats was investigated in PBS buffer solution at physiological temperature of 37°C for 3 day periods. Figure 4.5 shows the difference of water retention capacity and dissolution of both fiber mats. At initial time period (i.e., 15 min), the water retention of the neat eSF and surface-modified eSF occurred more rapidly when they were immersed in medium with the property value of surface-modified eSF being slightly lower than neat mats, i.e., 123.21 % and 77.62 % respectively. A further increase of submersion time resulted in an increase in the water retention of both types of fiber mats to finally become saturated at the equivalent property values after 24 h of submersion of 181.42 % and 180.19 % respectively. At the same time, dissolution of both fiber mats was observed along submersion time. The weight of both types of fibers slightly decreased along their submersion in PBS due to partial disintegration of fiber mat. In comparison, at initial submersion time of 15 min, the dissolution of

surface-modified eSF fiber mat was occurred rapidly which remaining weight was lower than the neat ones. After 3 days of submersion, the weight of neat and surface-modified eSF fiber mats were decreased to 93.93 % and 91.72 % respectively. It can be obviously observed that surface-modification was not effect to the dissolution behavior of the eSF fibers. The rapid dissolution rate of surface-modified eSF fiber mats may be due to partial disintegration which can be attributed by desorption of fibronectin proteins.

4.4.4 Indirect Cytotoxicity Evaluation

The biocompatibility of Thai silk fibroin fiber mat was evaluated on the cytotoxicity of these materials in this study since they were fabricated via electrospinning process with PEO, known toxic substance, in blending for preparation of silk fibroin into the electrospun fiber mats. Normal human dermal fibroblasts were used as reference in the assessment that had been cultured with extraction medium in comparison with fresh cultured media (i.e., control). The results are shown in Figure 4.6. Three extraction ratios of the extraction media (i.e., 5, 10, 20 mg/ml) were investigated. Evidently, both the neat and surface modified eSF fiber mats were non-toxic to the NHDF. The cell viability of NHDF was in the range of 84 % to 120 % based on the viability of the cells that had been cultured with fresh cultured medium. Interestingly, the viability of the cells for surface-modified eSF fiber mats was higher than the neat for all extraction ratios. With regards to the surface-modified eSF fiber mats, the viability of the cells cultured in the lowest extraction ratio (i.e., 5 mg/ml) from the fiber mats was ~120 %, which was significantly greater than that of the extraction medium from the neat one. Based on the results obtained, the extraction medium from both types of fiber mats did not released any harmful substance to the fibroblast. These materials could be further evaluated for their potential on wound healing

4.4.5 Cell Attachment and Cell Proliferation

Wound healing is a unique biological process which is related to many physiological parameters that automatically occur under normal condition [2]. Since the absence of cytotoxicity, the initial attachment and proliferation might be an important contributing factor for tissue remodeling. Both eSF fiber mats, which mimic a natural ECM, were studied as a supporting cell growth by using human

normal fibroblasts which are one of the most abundance cell types in connective tissue that function to maintain tissue homeostasis when tissues are injured [4]. Figure 4.7 shows the absorbance value signifying the viabilities of the cells that had been cultured on the surfaces of both eSF fiber mat and glass substrate (i.e., control). NHDF were seeded on the surface of these substrates for 2, 4, and 8 h. for the attachment study and 1, 2, and 3 day(s) for proliferation study. For Both types of eSF fiber mats, the viability of the attached cells increased monotonically with an increasing of culturing time (Figure 4.7a). At all of the culturing time point investigated, the viability of the cells that attached on the surface of both eSF fiber mats was significantly greater than the control which could be a result of the biocompatibility of the silk fibroin protein and the large surface area of nanofiber construction that is available for cell to attach. The attachment of the NHDF on the eSF fiber mats was further improved with the immobilization of fibronectin on the surface. For the proliferation study (Figure 4.7b), Interestingly, the surface-modified eSF fiber mats show greater cell viability in any culturing time point while the viability of the NHDF on the neat eSF fiber mat was less than that of the control after they had been cultured on the surface for 2 days. This could be due to the cells that might have proliferated priority in 2D direction which influence by the orientation of the fibers instead of 3D direction which the cells have to penetrate into the porous structure of the fibrous scaffold. The introduction of fibronectin onto the surface of eSF fibers could be induced the cells to proliferate inside the porous structure since fibronectin contain the cell- binding domain RGD, which have been known to play a critical role in cell behavior because they regulate gene expression by the signal transduction set by cell adhesion to a functional biomaterial.

4.4.6 Morphology of Cultured Cells

Table 2, 3 respectively show representative SEM images of attachment and proliferation activity of NHDF that was cultured on the surface of both types of eSF fibers mat and glass substrate at various culture time. According to Table 2, at 2 h after cell seeding, NHDF attachment on both types of eSF fiber mat and the glass substrate started to extend their filopodia, which are thin fiber-like cytoplasmic projections, to create their anchorage on the fiber surfaces. At 4 h and 8 h after cell seeding, the cells on both fiber mats and glass substrate further extended

their filopodia around the leading edge with strong evidence of lamellipodia while those on fibronectin-modified eSF fiber mat were the flattest in shape of migrating cells. The cells on both fiber mats were well extended with direction which might be created by the fibers in comparison to those on glass substrate that were still in round shape. During the proliferation period according to Table 3, evidently appeared on fibronectin-modified eSF fiber mat, the cells that had been seeded on all substrates were well expanded in their cytoplasm in the form of thin and long spindle-like shape at 1 day after cell culturing. By further increasing the culturing time to 2 and 3 days, the cells appeared in their typical spindle morphology and spreaded over the surface for all substrate. Interestingly, while the majority of the cells growth on the fibronectin-modified eSF fibers similarly assumed the spindle morphology as the others, the viability of the cells that had been cultured on these fibers surface was always greater than that on others substrate. As previously mentioned, Saturation of the viability of the cells might be due to the migration of the cells onto the hypothetical monolayer construct, even though they were on three dimensional scaffold. To investigate cell migration behavior, cross-section images of neat and surface-modified eSF fibers were further evaluated that shown in Figure 4.8. Prior to cell seeding, neat (Figure 4.8a) and surface-modified eSF fiber mat (Figure 4.8c) also show the bundle of fiber along the cross-section surface. Interestingly, 3 days after cell seeding, the fiber layer construction of the neat eSF mat was still observed on the cross-section of the eSF fiber mats (Figure 4.8a), while that of surface-modified eSF fiber mats were filled up the empty space which could be due to the propagation of the cells within the inner layer to form a three-dimensional connective tissue (Figure 4.8b).

4.5 Conclusions

This study explored a novel biomaterial-scaffold design to achieve the ultra-fine nanofibers with surface modification for bioactive wound dressing. Electrospun silk fibroin (eSF) was successfully fabricated from electropinning 70:30 weight ratio of SF:PEO, PEO with molecular weight of 600 kDa, in aqueous solution at RH<30%. These fibers mat had average diameters of the individual fibers that were

290±46 nm via PEO extraction which did not affect the morphology of the fiber mat. Fibronectin was used to immobilize by the carbodiimide chemistry method on the surface of eSF fiber mat. ATR-FTIR data confirmed the existence of the immobilized fibronectin, while the XPS spectra indicated the grafting efficiency that the O-C=O and C-(C,H) was significantly increased due to the coupling of fibronectin on the fiber surface. The potential used of neat and surface-modified eSF fiber mats as wound dressing or tissue-remodeling material was assessed with normal human dermal fibroblast (NHDF). Indirect cytotoxic evaluation revealed that both neat and modified eSF fiber mat released no substance that was harmful to the cells. Significantly, the surface-modified eSF fiber mat showed the greatest ability to support the attachment and proliferation of NHDF. Visual observation based on SEM revealed that NHDF penetrate well into the empty space of the fiber mat to form a three dimensional connective tissue. These results demonstrate that eSF mats with surface modification of fibronectin are of great interest for biomedical application especially for accelerated wound healing.

4.6 Acknowledgments

The authors acknowledge partial support received from (a) the National Nanotechnology Center (grant number: BR0108), (b) the National Center of Excellence for Petroleum, Petrochemicals, and Advanced Materials (NCE-PPAM), and (c) the Petroleum and Petrochemical College, Chulalongkorn University, Thailand. J. Chutipakdeevong acknowledges a doctoral scholarship received from the Thailand Graduate Institute of Science and Technology (TGIST) (TG-55-09-51-035D).

4.7 References

1. Ovington, L. *Clin. Dermatol.* **2007**, *1*, 33-38
2. Schreml, S.; Szeimies, R.-M.; Prantl, L.; Landthaler, M.; Babilas, P. *J. Am. Acad. Dermatol.* **2010**, *5*, 866-881

3. Zahedi, P.; Rezaeian, I.; Ranaei-Siadat, S.-O.; Jafari, S.-H.; Supaphol, P. *Polym. Adv. Technol.* **2009**, *21*, 77-95
4. Li, B.; Wang, J.H.C. *J. Tissue. Viabil.* **2011**, *20*, 108-120
5. Agarwal, S.; Wendorff, J.H.; Greiner, A. *Polymer* **2008**, *26*, 5603-5621
6. Alessandrino, A.; Marelli, B.; Arosio, C.; Fare, S.; Tanzi, M.C.; Freddi, G. *Eng. Life Sci.* **2008**, *3*, 219-225
7. Altman, G.H.; Diaz, F.; Jakuba, C.; Calabro, T.; Horan, R.L.; Chen, J.; Lu, H.; Richmond, J.; Kaplan, D.L. *Biomaterials* **2003**, *3*, 401-416
8. Hardy, J.G.; Scheibel, T.R. *Prog. Polym. Sci.* **2010**, *9*, 1093-1115
9. Vepari, C.; Kaplan, D.L. *Prog. Polym. Sci.* **2007**, *8-9*, 991-1007
10. Wadbua, P.; Promdonkoy, B.; Maensiri, S.; Siri, S. *Int. J. Biol. Macromol.* **2010**, *5*, 493-501
11. Zhou, C.-Z.; Confalonieri, F.; Medina, N.; Zivanovic, Y.; Esnault, C.; Yang, T.; Jacquet, M.; Janin, J.; Duguet, M.; Perasso, R.; Li, Z.-G. *Nucleic Acids Res.* **2000**, *12*, 2413-2419
12. Yang, M.; Kawamura, J.; Zhu, Z.; Yamauchi, K.; Asakura, T. *Polymer* **2009**, *1*, 117-124
13. Fan, H.; Liu, H.; Toh, S.L.; Goh, J.C.H. *Biomaterials* **2008**, *8*, 1017-1027
14. Hofmann, S.; Wong Po Foo, C.T.; Rossetti, F.; Textor, M.; Vunjak-Novakovic, G.; Kaplan, D.L.; Merkle, H.P.; Meinel, L. *J. Controlled Release* **2006**, *1-2*, 219-227
15. Jin, H. *Biomaterials* **2004**, *6*, 1039-1047
16. Kim, K.; Jeong, L.; Park, H.; Shin, S.; Park, W.; Lee, S.; Kim, T.; Park, Y.; Seol, Y.; Lee, Y. *J. Biotechnol.* **2005**, *3*, 327-339
17. Lee, E.-H.; Kim, J.-Y.; Kweon, H.Y.; Jo, Y.-Y.; Min, S.-K.; Park, Y.-W.; Choi, J.-Y.; Kim, S.-G. *Oral. Surg. Oral. Med. Oral. Pathol. Oral. Radiol. Endod.* **2010**, *5*, e33-e38
18. Meechaisue, C.; Wutticharoenmongkol, P.; Waraput, R.; Huangjing, T.; Ketbumrung, N.; Pavasant, P.; Supaphol, P. *Biomed. Mater.* **2007**, *3*, 181-188
19. Meinel, A.J.; Kubow, K.E.; Klotzsch, E.; Garcia-Fuentes, M.; Smith, M.L.; Vogel, V.; Merkle, H.P.; Meinel, L. *Biomaterials* **2009**, *17*, 3058-3067

20. Meinel, L.; Hofmann, S.; Karageorgiou, V.; Kirker-Head, C.; McCool, J.; Gronowicz, G.; Zichner, L.; Langer, R.; Vunjak-Novakovic, G.; Kaplan, D.L. *Biomaterials* **2005**, *2*, 147-155
21. Min, B.-M.; Lee, G.; Kim, S.H.; Nam, Y.S.; Lee, T.S.; Park, W.H. *Biomaterials* **2004**, *7-8*, 1289-1297
22. Schneider, A.; Wang, X.Y.; Kaplan, D.L.; Garlick, J.A.; Egles, C. *Acta Biomater.* **2009**, *7*, 2570-2578
23. Wang, Y.; Kim, H.-J.; Vunjak-Novakovic, G.; Kaplan, D.L. *Biomaterials* **2006**, *36*, 6064-6082
24. Zhang, X.; Baughman, C.B.; Kaplan, D.L. *Biomaterials* **2008**, *14*, 2217-2227
25. Zhang, X.; Reagan, M.R.; Kaplan, D.L. *Adv. Drug Delivery Rev.* **2009**, *12*, 988-1006
26. Zarkoob, S.; Eby, R.K.; Reneker, D.H.; Hudson, S.D.; Ertley, D.; Adams, W.W. *Polymer* **2004**, *11*, 3973-3977
27. Chen, C.; Chuanbao, C.; Xilan, M.; Yin, T.; Hesun, Z. *Polymer* **2006**, *18*, 6322-6327
28. Li, C.; Vepari, C.; Jin, H.-J.; Kim, H.J.; Kaplan, D.L. *Biomaterials* **2006**, *16*, 3115-3124
29. Bai, L.; Zhu, L.; Min, S.; Liu, L.; Cai, Y.; Yao, J. *Appl. Surf. Sci.* **2008**, *10*, 2988-2995
30. Richert, L.; Boulmedais, F.; Lavalle, P.; Mutterer, J.; Ferreux, E.; Decher, G.; Schaaf, P.; Voegel, J.-C.; Picart, C. *Biomacromolecules* **2003**, *2*, 284-294
31. Mattanavee, W.; Suwantong, O.; Puthong, S.; Bunaprasert, T.; Hoven, V.P.; Supaphol, P. *ACS Appl. Mater. Interfaces* **2009**, *5*, 1076-1085
32. Ahimou, F.; Boonaert, C.J.P.; Adriaensen, Y.; Jacques, P.; Thonart, P.; Paquot, M.; Rouxhet, P.G. *J. Colloid Interface Sci.* **2007**, *1*, 49-55.

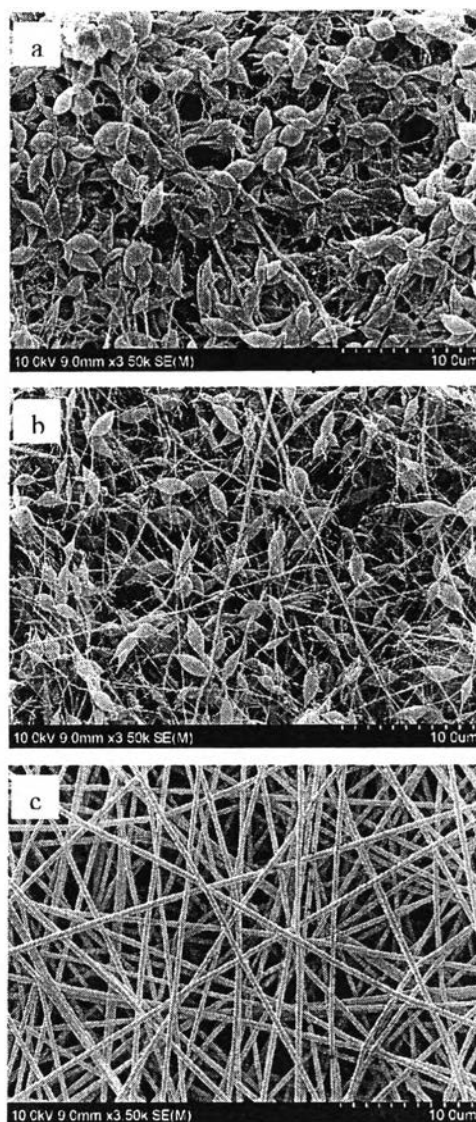


Figure 4.1 SEM micrographs of electrospun SF/PEO fibers at different humidity: (a) RH ~ 60%, (b) RH ~ 45% and (c) RH < 30%. Weight ratio of SF/PEO is 70:30 in 10 % (w/v) of aqueous.

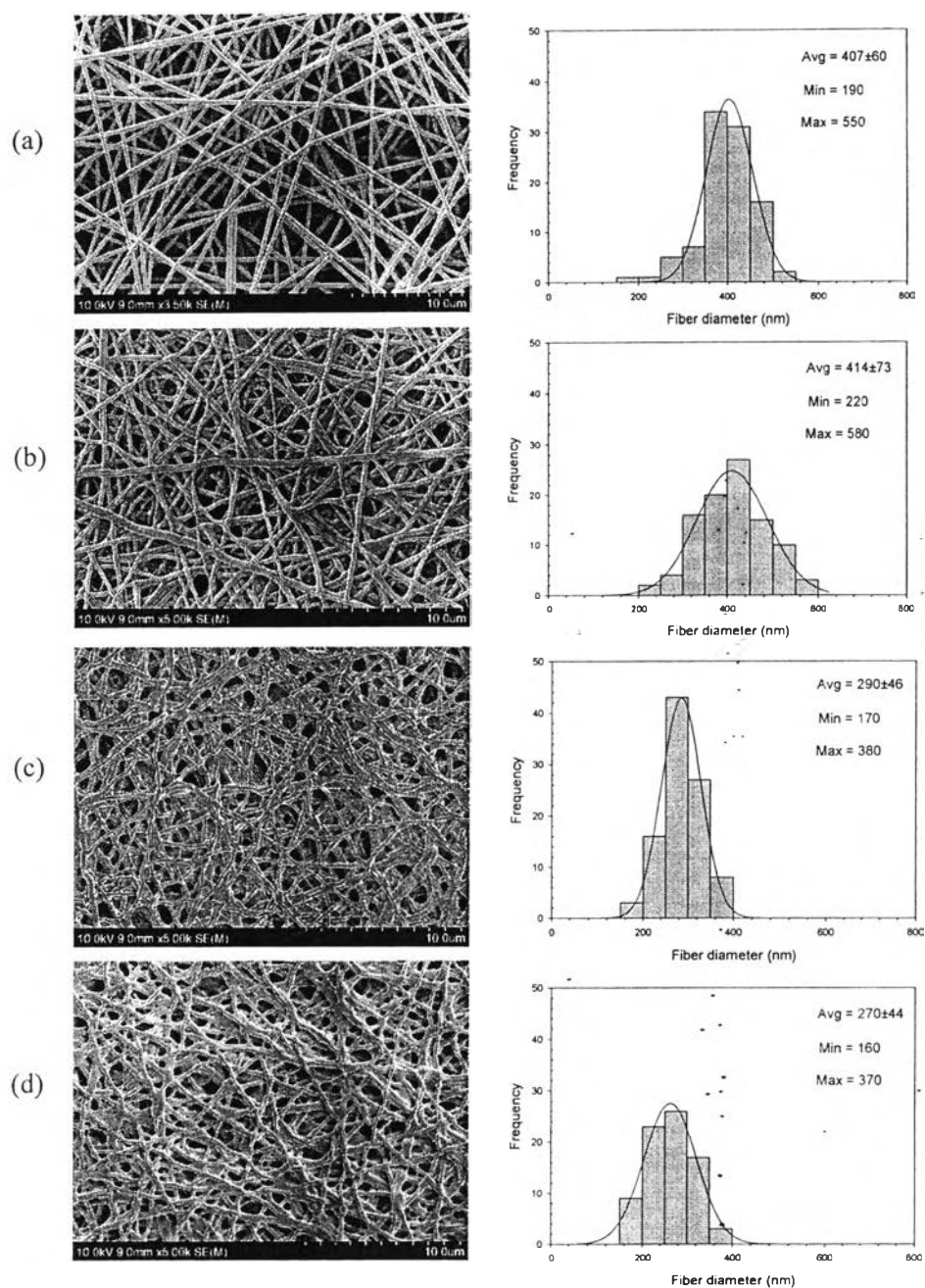


Figure 4.2 The morphology and fiber diameter at various states of electrospinning of silk fibroin nanofibers of: (a) electrospun SF/PEO fibers, (b) MeOH treated SF/PEO fibers, (c) eSF fibers after PEO extraction, and (d) surface-modified eSF fibers. Applied electric field strength was 14 kV/15 cm.

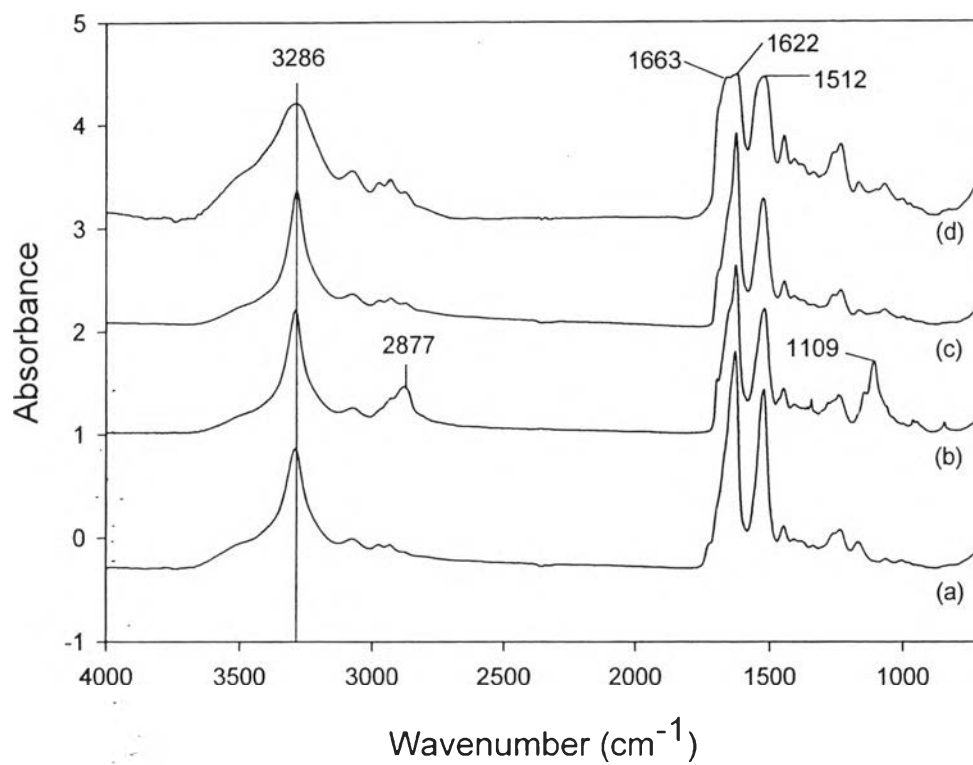


Figure 4.3 FTIR spectrums of different states silk fibroin proteins: (a) silk fibroin film, (b) electrospun SF/PEO fiber mat, (c) eSF fiber mat after PEO extraction, and (d) surface-modified eSF fiber mat.

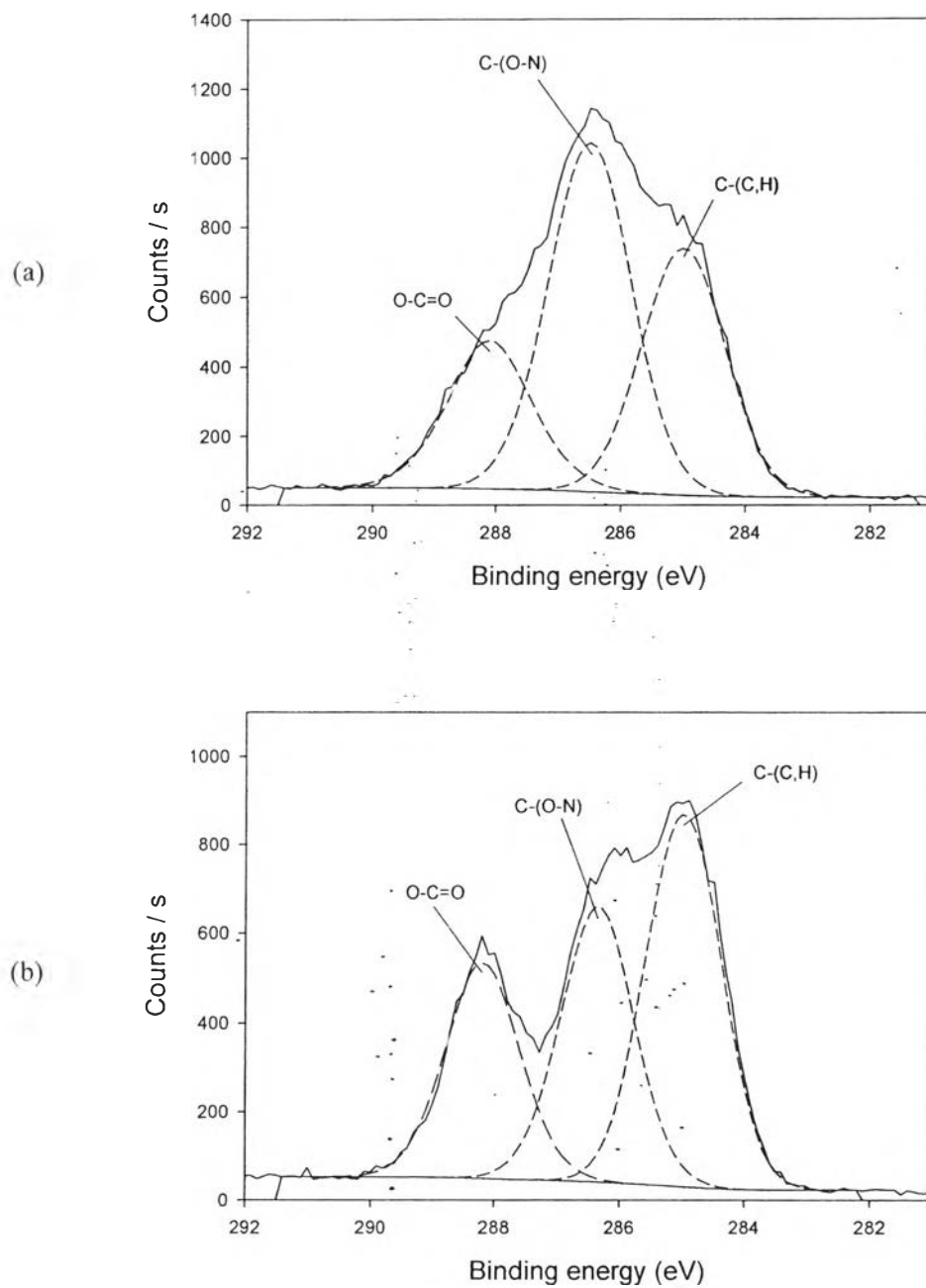


Figure 4.4 XPS photoelectron peaks of C 1s of: (a) eSF and (b) surface-modified eSF fiber mat. The different chemical compositions obtained from peak fitting are shown.

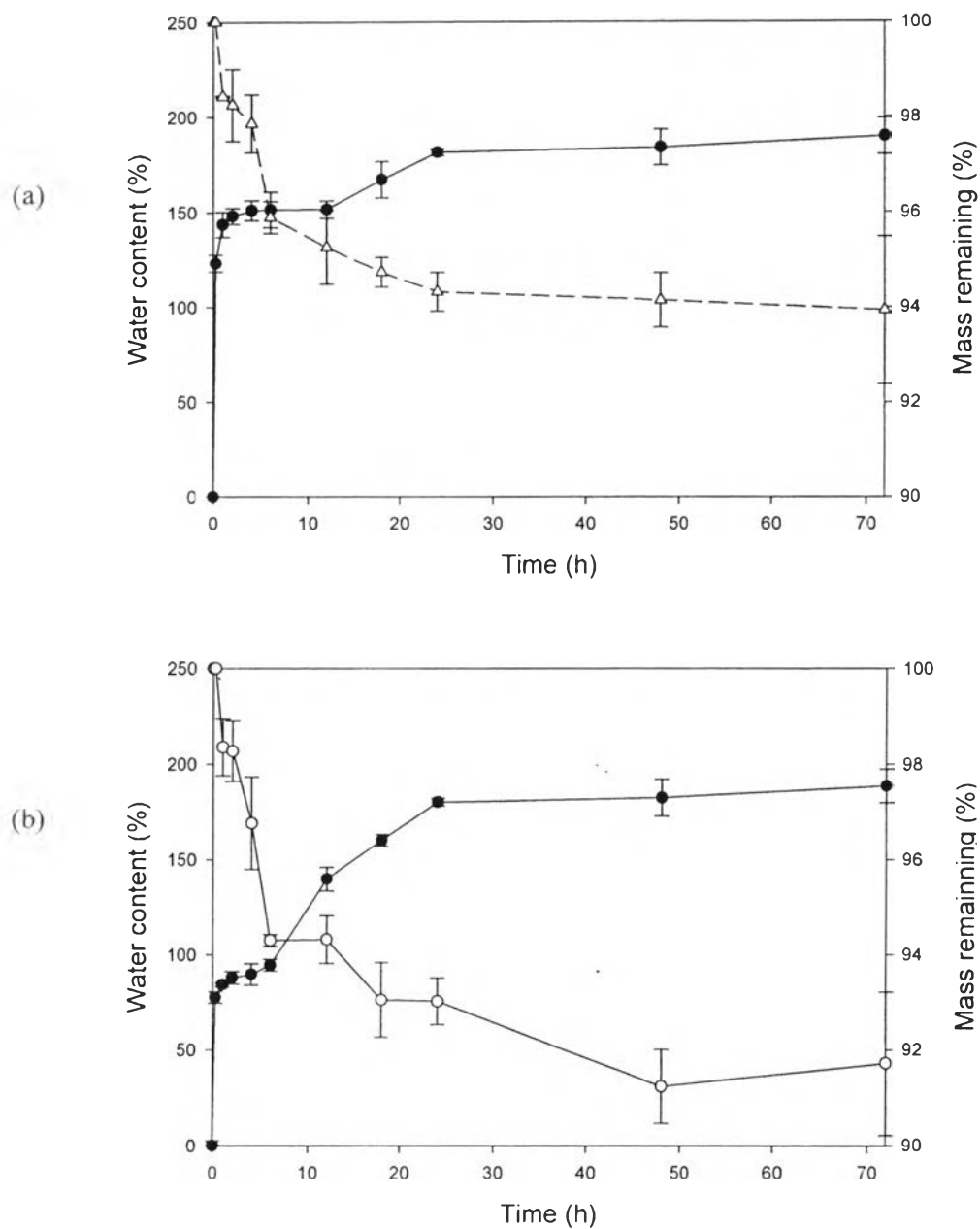


Figure 4.5 Water retention capacity (●) and dissolution (○) of: (a) eSF and (b) surface-modified eSF fiber mat at various time points in PBS buffer at 37 °C.

Table 4.1 XPS surface chemical compositions and elemental ratio of eSF fibers before and after modification with fibronectin

Sample	Surface atomic composition (at.%)			Elemental composition ratio		Chemical functions (at.%)				
	C 1s	N 1s	O 1s	N/C	O/C	285.0 ^a C-(C,H)	286.5 ^a C-(O,N)	288.1 ^a O-C=O	533.1 ^a C-O	531.9 ^a C=O
eSF fibers	67.4	9.5	23.2	0.14	0.34	22.3	31.5	13.7	12.4	10.7
Surface-modified eSF fibers	63.6	16.0	20.4	0.25	0.32	27.6	20.2	15.9	4.2	16.1

^a Binding energy (electron volts)

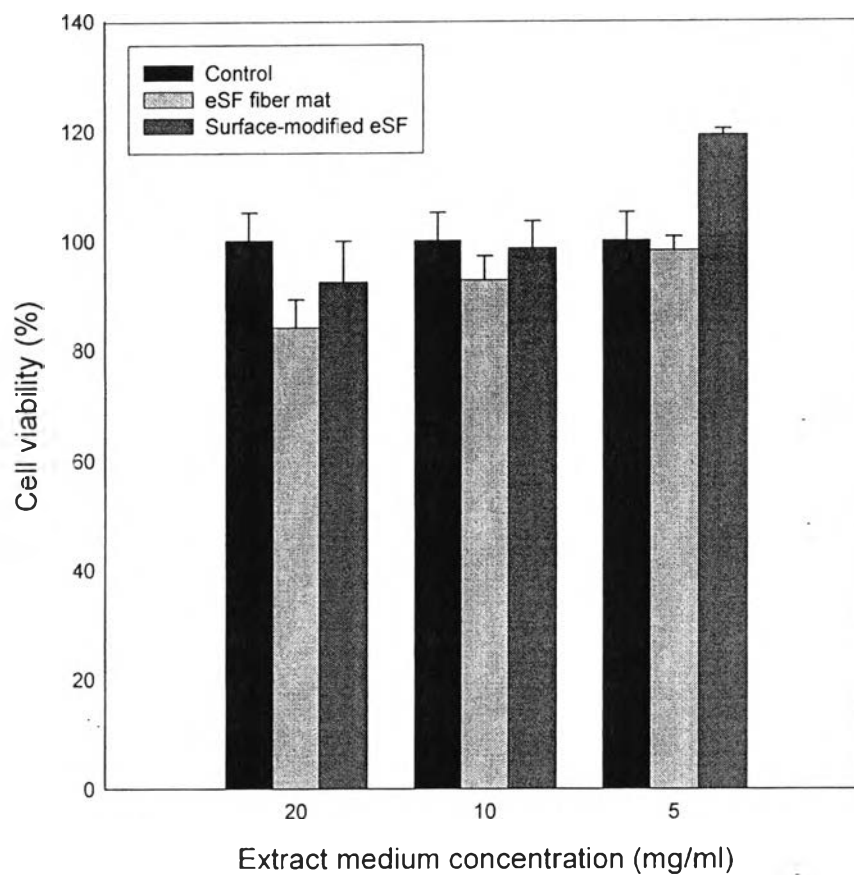


Figure 4.6 Indirect cytotoxicity evaluation of the neat and modified eSF fiber mat based on the viability of normal human dermal fibroblasts (NHDF) cultured with various extraction media concentration for 24 hours.

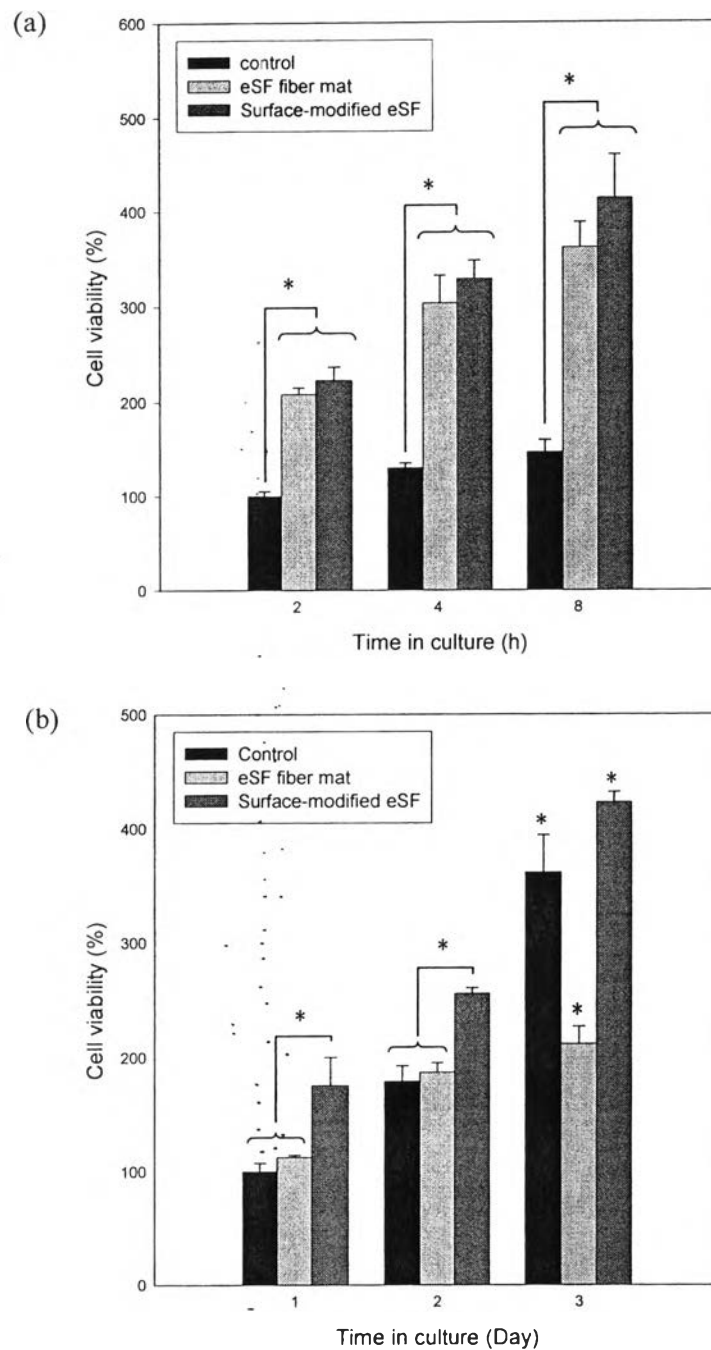


Figure 4.7 Cell viability of NHDF (a) attachment and (b) proliferation. The NHDF were either seeded or cultured on control, eSF fiber mat, and surface-modified eSF fiber mat as a function of time

Table 4.2 SEM images of human dermal fibroblasts (NHDF) attachment on glass slide (i.e., control), electrospun silk fibroin fibers (eSF) and surface-modified eSF fibers for 2 h, 4 h and 8 h. (magnification = 500x)

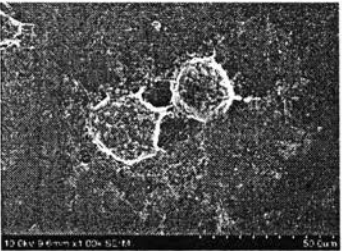
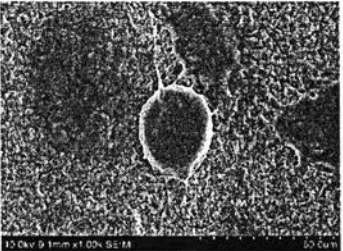
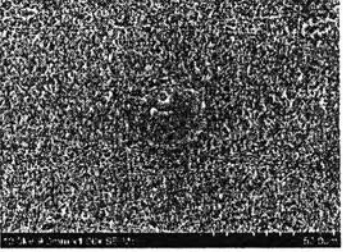
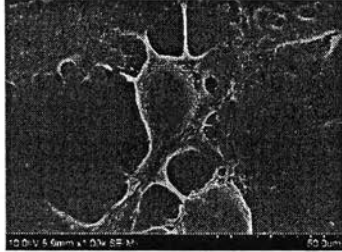
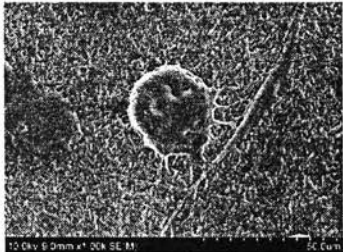
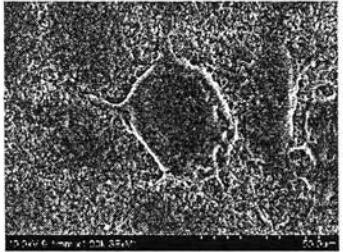


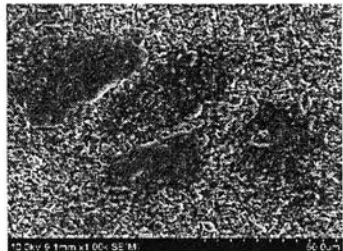
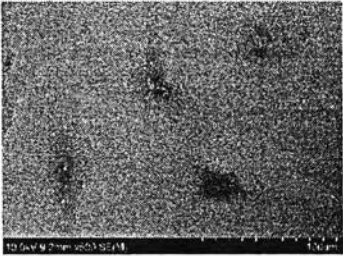
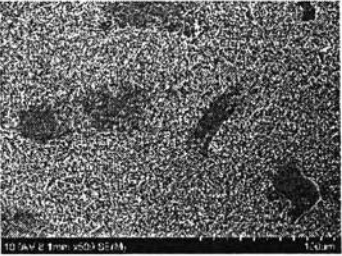
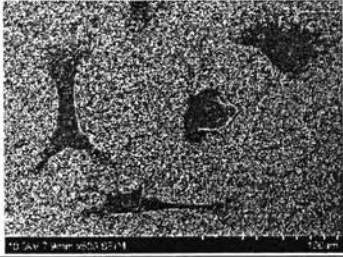
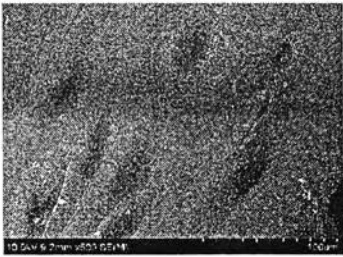
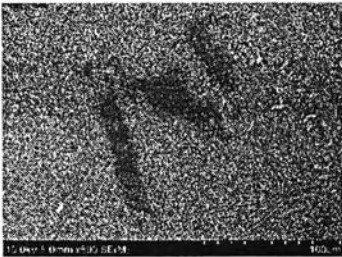
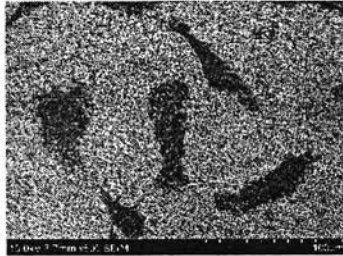
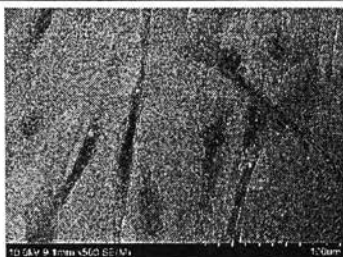
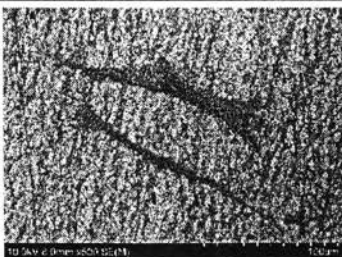
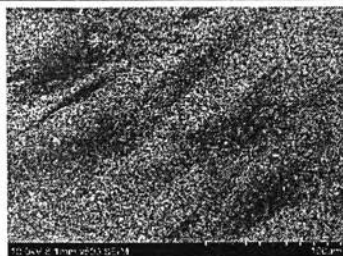
Culturing time	Type of substrate		
	Glass	eSF fibers	Surface-modified eSF fibers
2 h			
4 h			
8 h			

Table 4.3 SEM images of human dermal fibroblasts (NHDF) proliferation cultured on glass slide (i.e., control), electrospun silk fibroin fibers (eSF) and surface-modified eSF fibers for 1 d, 2 d and 3 d (magnification = 1000x)

Culturing time	Type of substrate		
	Glass	eSF fibers	Surface-modified eSF fibers
1 d			
2 d			
3 d			

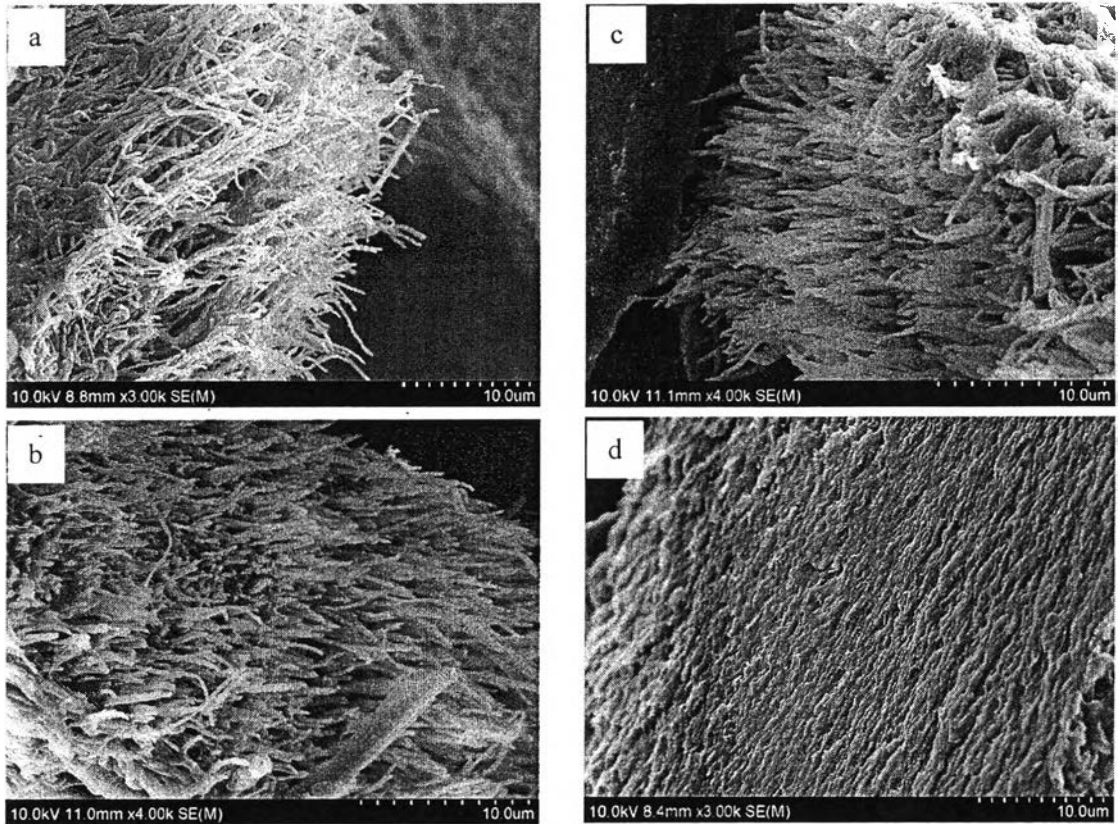


Figure 4.8 Cross-section images of: (a,b) neat eSF fibers mat and (c,b) surface-modified eSF fibers mat before and after cell culture for 3 days respectively (magnification = 3000x)